

Surface polarization strongly influences electrostatics in a nonlocal medium

Ali Behjatian,¹ Ralf Blossey,² and Madhavi Krishnan^{1,3, a)}

¹⁾ *Physical and Theoretical Chemistry Laboratory, Department of Chemistry, University of Oxford, South Parks Road, Oxford OX1 3QZ, UK.*

²⁾ *Université de Lille, Unité de Glycobiologie Structurale et Fonctionnelle (UGSF), CNRS UMR8576, 59000 Lille, France*

³⁾ *The Kavli Institute for Nanoscience Discovery, Sherrington Road, Oxford OX1 3QU, UK.*

Electrostatics in the solution phase is governed by free electrical charges such as ions, as well as by bound charges that arise when a polarizable medium responds to an applied field. In a local medium, described by a constant dielectric permittivity, the sign of the far-field electrostatic potential distribution around an object is governed by its electrical charge. We demonstrate significant departures from this expectation in a nonlocal medium characterized by a wave vector-dependent dielectric function. Here, surface polarization due to the solvent, or indeed non-solvent dipoles, may wield significant influence at large distances. The polarization correlation length may not only significantly augment the effective screening length, but we show that the electrical contribution from polarization can compete with and even invert the sign of the electrical potential and the field arising from charge alone. These results hold ramifications for a range of apparently anomalous electrically governed observations such as underscreening, electrophoretic mobilities of charge-neutral objects, and long-ranged attraction between like-charged entities in water and other solvents.

I. INTRODUCTION

Interactions between charge-carrying molecules and particles in the fluid phase form the bedrock of collective processes underpinning chemistry and biology. In media of high dielectric constant such as water, and in the presence of low concentrations of monovalent salt ions, the Poisson-Boltzmann (PB) theory is believed to provide an accurate description of electrostatic interactions. A hallmark of PB-theory is the expectation of a repulsive force between electrically like-charged entities that decays with increasing separation at a rate given by the Debye screening length, $\kappa^{-1} = 1/\sqrt{8\pi n_0 \ell_B}$. Here, n_0 is the bulk number density of positive or negative monovalent ions in solution, and $\ell_B = e^2/4\pi\epsilon_0\epsilon_s k_B T$ is the Bjerrum length, where e , ϵ_0 , ϵ_s , k_B , and T , denote the elementary charge, permittivity of free space, static dielectric constant of the medium, Boltzmann's constant, and absolute temperature, respectively. Many important indications of PB theory have indeed been captured in a range of mechanical force measurement experiments¹⁻³. However, there have been wide-ranging experimental reports of departures from PB theory, mainly centered on interactions inferred from the spatial structure of suspensions of particles and molecules probed using visible light and x-rays⁴⁻¹⁰. Furthermore, interesting observations persist concerning electrokinetic mobility of neutral lipid vesicles, as well as long-ranged attraction measured for net-neutral lipid bilayer coatings^{11,12}.

The canonical theoretical view of electrostatic interactions entails treating a fluid as a local continuum described by a phenomenological electric susceptibility con-

stant, $\chi \geq 0$, with the solvent merely providing a structureless shielding background¹³. The susceptibility constant, χ , establishes a linear relationship between the polarization, \mathbf{P} , and the electric field, \mathbf{E} – i.e. $\mathbf{P} = \epsilon_0 \chi \mathbf{E}$. Far from a structureless continuum, however, fluid media are in fact grainy. The structure is sustained by short-range intermolecular interactions such as dipole-dipole interactions and hydrogen bonding, but may also display long-range orientational correlations according to several experimental reports¹⁴⁻¹⁸. Indeed the incorporation of a description of intermolecular interactions led to successful modeling of the short-range hydration force, which was first experimentally observed in the 1980s^{19,20}. Here we construct a model of electrostatics in a medium capable of sustaining molecular orientational correlations that decay over a distance ξ – the polarization correlation length. We examine the consequences thereof on the electrostatic far-field, defined by distances 2–3 times larger than the Debye length, the relevant length scale in a local medium or electrolyte.

A significant simplification at the heart of local continuum electrostatic theories posits that the response of the medium, \mathbf{P} , may not depart from that dictated by the disturbance, \mathbf{E} . Accordingly, the polarization surface charge, defined as $\sigma_p = \mathbf{P} \cdot \mathbf{n}$, where \mathbf{n} is the normal vector directed outward to the dielectric material (Fig. 1), is determined self-consistently from Gauss' law and cannot be treated as an independent parameter of the system. Molecular dynamics (MD) simulations however reveal the presence of oriented solvent dipoles in the vicinity of neutral surfaces/interfaces immersed in a variety of polar solvents²¹⁻²⁴. This occurs presumably due to anisotropic bonding interactions of solvent molecules located at a discontinuity and can entail substantial magnitudes of net polarization, $P \approx 0.1e \text{ nm}^{-2}$, even at a neutral surface carrying no electrical charge, immersed, e.g.,

^{a)} Electronic mail: madhavi.krishnan@chem.ox.ac.uk

in water. Such behavior has also been extensively confirmed in nonlinear spectroscopy experiments on water at interfaces^{25–28}. This net orientation of solvent molecules at interfaces thus implies an “excess” interfacial polarization which has been suggested to play an important role in interparticle interactions, but the effects of which cannot be completely and self-consistently captured within the local electrostatic view²⁴.

In contrast, a nonlocal medium permits the polarization \mathbf{P} to depart from \mathbf{E} over distances where polarization correlations are non-negligible. A discontinuity in the polarization across the interface, arising e.g., from anisotropy in solvent bonding interactions, produces a polarization surface charge, σ_p . In an ion-free nonlocal medium, the polarization surface charge couples into that in the bulk. This generates a spatial polarization profile and concomitant electric field whose decay is governed by the polarization screening length $\lambda \propto \xi$. Thus for an object immersed in an electrolyte, even in the absence of charge on the object, an electrical double layer may form. When $\lambda \gtrsim \kappa^{-1}$, the effective extent of the resulting counterion cloud can depart significantly from that given by κ^{-1} characteristic of a local medium. Furthermore, in the presence of both surface charge density, σ , and polarization charge density σ_p , coupling of the two sources results in an overall net electric field whose sign, magnitude, and spatial rate of decay are sensitively governed by the values of the underpinning system parameters, as discussed in detail in what follows. Importantly, λ and ξ are in general not identical, and the relationship between these quantities strongly depends on the form of the dielectric function which describes the nonlocal response of the medium. While the determination and implementation of the exact form of dielectric function is a non-trivial task^{29–31}, the use of a Lorentzian approximation can lead to a significant simplification of the model³² and a linear relationship between λ and ξ : i.e., $\lambda = \xi\sqrt{\theta}$. Here, $\theta = \epsilon_s/\epsilon_\infty$ is the ratio of the static dielectric constant of water, $\epsilon_s \approx 80$, to a value $\epsilon_\infty \approx 2\text{--}5$ at frequencies just above the first dispersion beyond which the rotational modes are effectively frozen.

II. MODEL

In the present study, we describe the consequences of this view based on a straight-forward generalization of PB-theory. We consider the impact of interfacial solvent polarization and embedded interfacial dipoles on the electrostatic far-field of an isolated charged plane in contact with a nonlocal electrolyte. The implications of an excess interfacial polarization for far-field electrostatics in nonlocal media have to our knowledge not been extensively explored, especially in the nonlinear regime where the Debye-Hückel (DH) approximation breaks down. We examine the results of the two-field formulation of nonlocal electrostatics proposed in Refs. 33 and 34 for surfaces carrying electrical charge σ in combination with

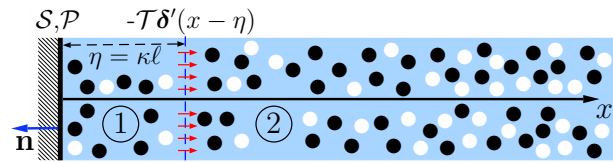


FIG. 1. Schematic representation of an infinite flat plate carrying electrical charge and polarization charge densities given by \mathcal{S} and \mathcal{P} respectively, in contact with a semi-infinite nonlocal electrolyte containing cations and anions. A negative value of \mathcal{P} corresponds to a polarization P in the positive x -direction. A layer of dipoles of density \mathcal{T} may be embedded at $x = \eta$ (red arrows).

(1) a surface polarization charge, σ_p , and (2) a dipole layer of surface density, τ , embedded in the interfacial region at a distance ℓ from the surface (see Fig. 1). The latter case may be taken to describe zwitterionic lipid headgroups, typically encountered in lipid monolayers or bilayers, or zwitterionic surface coatings. Here we only consider the role played by charges that describe the embedded dipoles and do not attempt to explicitly capture solvent polarization around the charged groups. We solve the governing equations adapted from Ref. 34 in the following dimensionless form,

$$-\frac{d^2\psi}{dx^2} = \rho \quad (1)$$

$$\delta^2 \frac{d^2\phi}{dx^2} = \theta(\phi - \psi) - \theta\delta^2\rho \quad (2)$$

for a semi-infinite domain $x > 0$ subject to the following boundary conditions: (i) $\psi'(0) = -\mathcal{S}$, (ii) $\phi'(0) = -\theta(\mathcal{S} + \mathcal{P})$, (iii) $\psi'(x) \rightarrow 0$ as $x \rightarrow \infty$, and (iv) $\phi'(x) \rightarrow 0$ as $x \rightarrow \infty$ (see Supplemental Material). In this formulation, the electric field, \mathbf{E} , and the displacement field, \mathbf{D} , are determined by the gradients of potential fields ϕ and ψ , respectively; i.e. $\mathbf{E} = -\nabla\phi$, $\mathbf{D} = -\nabla\psi$. Moreover, in our non-dimensional setup, ϕ is equivalent to the electrical potential expressed in units of $k_B T/e$ (see Supporting Material). Here, the dimensionless quantities $\mathcal{S} = 2\text{sgn}(\sigma)/\kappa\ell_c$ and $\mathcal{P} = 2\text{sgn}(\sigma_p)/\kappa\ell_p$ reflect the surface charge, σ , and the polarization charge, σ_p , through the ratios of the Debye length, κ^{-1} , to their corresponding Gouy-Chapman lengths, $\ell_c = e/2\pi|\sigma|\ell_B$ and $\ell_p = e/2\pi|\sigma_p|\ell_B$, respectively. Furthermore, the function $\rho = -\sinh\phi - \mathcal{T}\delta'(x - \eta)$ represents the sum of charge density arising from the free ions in the system (the first term) as well as from the dipole layer embedded at $\eta = \kappa\ell$ represented by the derivative of a Dirac δ -function (the second term). Finally the dimensionless quantity $\mathcal{T} = 4\pi\tau\ell_B/e$ describes the surface dipole density of the dipole layer. The above rescaling demonstrates that the problem may be cast in the form of an interplay between several characteristic length scales. Importantly, the parameter $\delta = \kappa\lambda$, which is the ratio of the polarization screening length, λ , to the Debye screening length,

κ^{-1} , captures the degree of nonlocality in the medium. In the limit $\delta \rightarrow 0$, the solution to Eqs. (1)-(2) converges to that of the standard PB equation that describes electrostatics in a local medium.

III. RESULTS AND DISCUSSION

We explore the role of polarization and dipoles embedded near a surface in nonlocal medium by considering two cases: (1) $\mathcal{P} \neq 0$; $\mathcal{T} = 0$ and (2) $\mathcal{P} = 0$; $\mathcal{T} \neq 0$, respectively. For small electrical potentials, $\phi \ll 1$, the solution of Eqs. (1)-(2) can be expressed in closed form³⁴. Using the Debye-Hückel approximation, $\rho \approx -\phi - \mathcal{T}\delta'(x - \eta)$, we find that the electrical potential, $\phi(x)$, has a double-exponential form

$$\phi(x) = A_+ \exp(-\kappa_+ x) + A_- \exp(-\kappa_- x), \quad (3)$$

where

$$\kappa_{\pm} = \left[\frac{\theta(1 + \delta^2)}{2\delta^2} \left(1 \pm \sqrt{1 - \frac{4\delta^2}{\theta(\delta^2 + 1)^2}} \right) \right]^{1/2} \quad (4)$$

represent dimensionless forms of two effective screening lengths $\kappa_{1,2} = \kappa\kappa_{\pm}$ that arise on account of the coupling between polarization charges and ions. In the absence of interfacial dipoles ($\mathcal{T} = 0$), Eq. (3) is valid over the entire domain $x \geq 0$. In the presence of the dipole layer however, the above equation is valid only in the region $x \geq \eta$. Accordingly, the coefficients A_+ and A_- are given by

$$A_i = \kappa_i \left(\frac{(\theta - \kappa_j^2)[S + \mathcal{T}\kappa_i \sinh(\eta\kappa_i)] + \theta\mathcal{P}}{\kappa_i^2 - \kappa_j^2} \right) \quad (5)$$

where $i, j \in \{+, -\}$ and $i \neq j$. Since $\kappa_+ > \kappa_-$, the coefficient A_- determines the electrical potential at long range and is a function of system parameters $(\mathcal{S}, \mathcal{P})$ or $(\mathcal{S}, \mathcal{T})$. In the nonlinear regime, where Eqs. (1)-(2) can only be solved numerically, we investigate the behavior of different systems by examining values of the effective surface potential ϕ_s determined by fitting an exponential function $\phi(x) = \phi_s \exp(-\kappa_- x)$ to the far-field of numerically calculated potentials $\phi(x)$. In the DH regime, we have $\phi_s = A_-$, as given by Eq. (5).

In general the dependence of ϕ_s on a pair of parameters $(\mathcal{S}, \mathcal{P})$ or $(\mathcal{S}, \mathcal{T})$ may be visualized as two-dimensional contour plots which reveal interesting trends. First, for $\mathcal{P} \neq 0$; $\mathcal{T} = 0$ (dipole layer absent), we observe that in the DH regime, the contourlines of A_- are described by parallel straight lines and the zero-level contour, given by $\mathcal{P} = (\kappa_+^2/\theta - 1)\mathcal{S}$, divides the \mathcal{S} - \mathcal{P} plane into two regions of positive and negative effective surface potentials (Fig. 2). When $\delta \rightarrow 0$, this line coincides with the \mathcal{P} -axis capturing the independence of A_- from \mathcal{P} (Fig. 2a). This behavior is characteristic of a local medium where the sole contribution to the far-field electrical potential

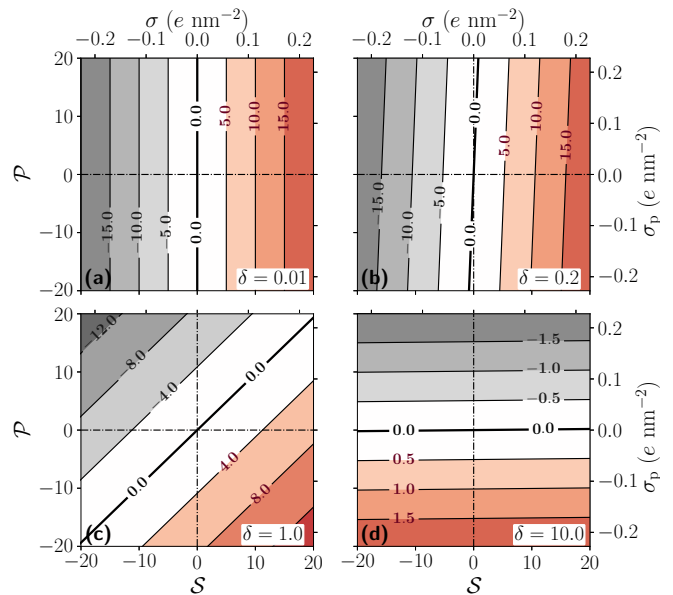


FIG. 2. Contours of effective surface potential, $\phi_s = A_-$, for the $(\mathcal{S}, \mathcal{P})$ problem in DH regime calculated using a Bjerrum length of $\ell_B \approx 0.7$ nm, characteristic of water at 298 K, and Debye screening length $\kappa^{-1} = 10$ nm.

stems from electrical charge, as intuitively expected. As δ grows in magnitude however, the zero-level contour rotates clockwise about the origin, and the interfacial polarization begins to contribute significantly to the far-field electrical potential. At intermediate values of δ there exist regions of the parameter space where the surface polarization, \mathcal{P} , can compete with surface charge, \mathcal{S} , and even invert the sign of the effective surface potential ϕ_s (Fig. 2). For $\delta \gg 1$, ϕ_s becomes independent of \mathcal{S} , and the behavior of the system in the far-field is purely determined by the polarization surface charge density, \mathcal{P} , which is diametrically opposite to behavior encountered in a local medium. While the above analysis provides qualitative insight into the impact of nonlocal effects on electrical potentials in electrolytes, the magnitude of the effective surface potential, A_- , in Fig. 2 implies that in general the problem lies significantly outside the regime of the validity of the DH approximation, $\phi \ll 1$. We therefore examine the problem in the nonlinear regime by numerically solving Eqs. (1)-(2).

The results of the analysis in the nonlinear regime reveal trends that are qualitatively comparable to the linear regime but more multifaceted in general. In the local limit ($\delta \rightarrow 0$), the non-uniform density of contourlines of fixed step size reflects the emergence of nonlinearity as \mathcal{S} increases (Fig. 3a). As δ grows, a substantial change in the shape of zero-level contour leads to a significant change in the far-field behavior. For $\delta \geq 0.2$ and a wide range of \mathcal{S} values, the sign of the far-field electrical potential depends sensitively on the value of \mathcal{P} (Fig. 3). In fact, for reasonable values of both \mathcal{S} and \mathcal{P} ($|\sigma|$ and

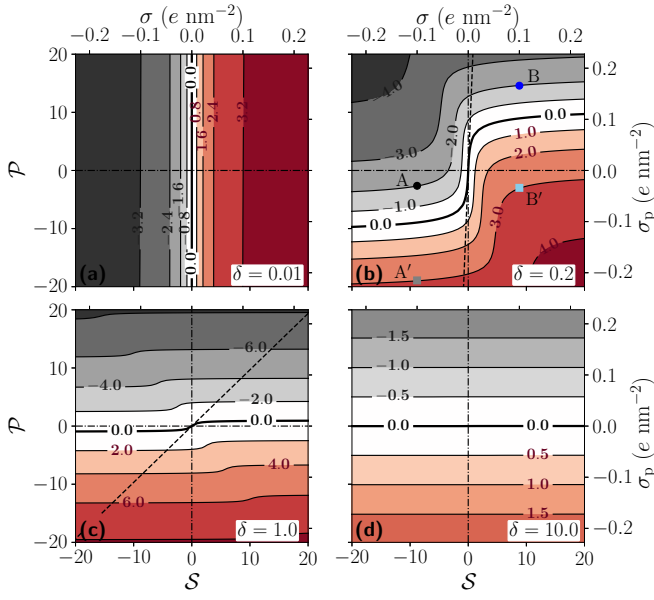


FIG. 3. Contours of effective surface potential, ϕ_s , for the (S, P) problem in the nonlinear regime, calculated using a Bjerrum length of $\ell_B \approx 0.7$ nm, characteristic of water at 298 K, and Debye screening length $\kappa^{-1} = 10$ nm. Dashed lines in (b) and (c) depict the zero-level contour in the DH regime.

$|\sigma_p| \approx 0.1e/\text{nm}^2$) the sign of the potential can be *opposite* to that expected based on the electrical charge alone.

To emphasize this point, we consider systems on either side of the zero-contour line in a pairwise fashion, e.g., characterized by points A, A', B and B' in the parameter space (Fig. 3b). First we consider pairs of systems (A, A') and (B, B') such that within each pair, S is identical both in sign and magnitude; i.e. $S_A = S_{A'}$ and $S_B = S_{B'}$. Furthermore the magnitudes of the effective surface potential, $|\phi_s| \approx 2-3$, are also comparable. However, importantly, the signs of ϕ_s are opposite in each pairing. Figure 4a displays the spatial variation of $\phi(x)$ together with their corresponding single exponential fits used to determine ϕ_s . Similarly, pairs of systems given by points (A', B') and (A, B) are characterized by opposite signs of charge density, S , and therefore display different $\phi(x)$ profiles at short-range. But within each pair, the spatial electrical potential profiles are essentially indistinguishable in the far field. Taken together, the above observations imply that electrically like-charged objects may appear oppositely charged in the far-field, and equally, that oppositely charged entities may appear like-charged at large separations (Fig. 4).

Finally, we examine the far-field surface electrical potential, ϕ_s , in case (2), $T \neq 0$, $P = 0$, in the $(S-T)$ plane for a dipole layer embedded near an interface in the electrolyte. This problem has been previously considered in the linear regime and the contribution of the dipoles to the far field was found to be negligible^{35,36}. This is in

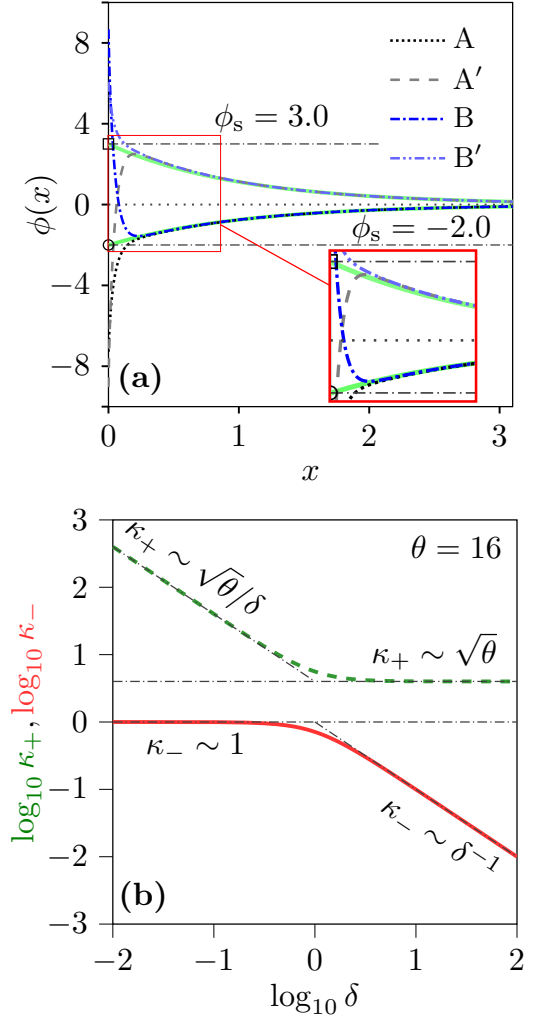


FIG. 4. (a) Profiles of electrical potential, $\phi(x)$, for points A, A', B, and B' indicated in Fig. 3b. Solid green lines represent fits to the far-field potential profile $\phi(x) = \phi_s \exp(-\kappa_+ x)$ where $\kappa_{\pm} = \kappa_{\text{eff}}$ represents the effective screening length. (b) Dependence of the two screening lengths, κ_{\pm} , on the non-locality parameter, δ , calculated for $\theta = 16$.

sharp contrast to our results on a system described by a *polarization* boundary condition, described above.

Equation (5) reveals a marked distinction between the (S, P) and (S, T) problems in the DH regime. Mainly we find that, holding all other parameters constant, the contribution of a dipole layer to the effective surface potential vanishes entirely as $\eta \rightarrow 0$. This behavior, common to both local and nonlocal media³⁵, implies that the influence of a dipole layer can only propagate into the far-field when it is embedded in the electrolyte rather than located at the surface ($\ell = 0$).

Investigating the problem in the nonlinear regime for $\eta = 0.05$ (corresponding to $\ell = 0.5$ nm and $\kappa^{-1} = 10$ nm), we find that an interfacial dipole layer can indeed make a tangible contribution to the far field for $\delta \gtrsim 0.2$,

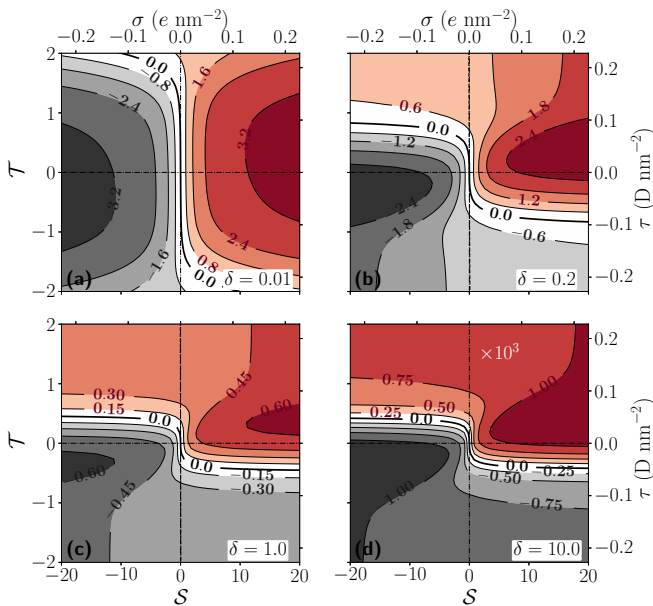


FIG. 5. Contours of effective surface potential, ϕ_s , for the (S, T) problem in nonlinear regime calculated using a Bjerrum length of $\ell_B \approx 0.7$ nm, characteristic of water at 298 K, and Debye screening length $\kappa^{-1} = 10$ nm. The dipole layer is located at $\eta = 0.05$. ϕ_s in (d) has been multiplied by a factor of 10^3 .

similar to the situation with a polarization boundary condition (see Fig. 5). But the trends observed for interfacial dipoles do reflect important quantitative differences to the polarization case that are most significant in the regime of $\delta \gg 1$. Here, surprisingly, neither the electrical charge nor electrical dipoles contribute to the electrical potential which nearly vanishes in the far-field. This result may be best understood by performing an asymptotic analysis in the linear regime which reveals that A_- decreases rapidly as $\delta \rightarrow \infty$ (see Supplemental Material).

IV. CONCLUSION

A central finding of our work is the unexpected role of the polarization boundary condition in influencing the sign of the electrical potential in the far field, as illustrated in our discussion of Figs. (3) and (4). This observation may have important ramifications for the counterintuitive and apparently anomalous experimental reports of “like-charge attraction” in the literature over the last several decades. By the same token, “opposite-charge repulsion” may also be expected. Thus attraction between non-identical but electrically like-charged objects in fact emerges as a natural consequence of this theoretical view, for experimentally meaningful values of all parameters. These results also support the possibility of experimentally observing non-zero electrophoretic mobil-

ities as well as far-field attraction or repulsion for electrically net charge-neutral objects and surfaces^{11,12,37}.

A key result of nonlocal models^{34,36,38–42} is the existence of two inverse screening lengths, $\kappa_{1,2}$, both of which depend on the length scale $\lambda = \xi\sqrt{\theta}$ where $\sqrt{\theta} \approx 4–9$ in the present approach (see Supplemental Material). Given the significant influence of λ on both the qualitative behavior of the electrical potential as well as the magnitude of the overall effective screening length in the far-field, an examination of the microscopic sources and mechanisms that govern the value of ξ is central to an assessment of the importance of nonlocal effects in practical contexts. Models of nonlocal electrostatics have traditionally attributed a variety of underpinning physical sources to the length scale ξ . These range from the most obvious: the length scale of molecular rotational correlations given by the intermolecular separation of 2–3 Å, to distances derived from interfacial dipole layer separations (≈ 1.5 Å)⁴¹, or the density of Bjerrum defects that act as sources and sinks of the polarization field in the medium (≈ 33 nm for ice)³⁸. Based on a value of $\xi \approx 3$ Å expected to describe pure bulk water, λ would not be expected to exceed 2–3 nm, which aligns reasonably well with literature estimates^{33,41,43}. This would in turn imply the onset of nonlocality given by, e.g., $\delta > 1$, and symbolized by (1) the departure of κ_{eff}^{-1} from the Debye screening length κ^{-1} , possibly accompanied by (2) flipping of the sign of the far-field electrical potential, at concentrations as low as 10 mM of monovalent salt ($\kappa^{-1} \approx 3$ nm).

Interestingly, nonlinear spectroscopy measurements of the decay length scale of polarization fluctuations in aqueous media have reported values as high as $\xi = 20$ nm in water¹⁶, 3–5 nm in electrolytes^{15–17}, and much larger for polyelectrolytes in solution¹⁸. The same is true for a range of apolar media where hyper-Rayleigh light scattering measurements suggest approximate lengths scales of 40 nm¹⁴ arising from phonon modes in the medium. The source of these correlations in water – whether they arise from poorly understood properties of the hydrogen bonding network or simply from the electric field due to ions in solution – remains unclear⁴⁴. Regardless of their origin, polarization correlation lengths of $\xi \approx 5–25$ nm in water would imply polarization screening lengths, $\lambda \gtrsim 50$ nm, which if true, would entail significant repercussions in experiments. For instance at salt concentrations higher than 0.1 mM, where $\kappa^{-1} < 30$ nm, $\lambda \sim 50$ nm entails $\delta \gtrsim 1$, implying that electrostatics can be significantly nonlocal under most experimentally relevant conditions. This entails not only significantly longer effective screening lengths but also possible inversion in sign of the measured far-field electrical potential.

The discussion on the origins and value of ξ would not be complete without insight from earlier reports, and specifically a recent MD simulation study on the related problem of short-ranged hydration forces in lipid bilayer systems^{20,45–47}. Netz *et al.* have suggested that laterally inhomogeneous water ordering can introduce a surface structural wavelength that may influence the overall

range of these short-range forces. Under the naïve assumption of translational invariance of surface properties (a homogeneous surface), such length scales – measured or inferred from experiments or from molecular simulations – would tend to be attributed to the properties of bulk water. If the polarization correlation and/or screening length is not solely governed by the properties of the bulk fluid there may not be grounds to expect ξ to be strictly limited to the rather small value given by the intermolecular separation of bulk solvent molecules. Although our present framework is concerned solely with a laterally averaged, homogeneous dipolar polarization density normal to the surface as the relevant structural order parameter in a Landau-Ginzburg formulation, higher order multipole densities, as well as their curls and gradients, may also contribute to the electrical potential on similar footing, each accompanied by an additional characteristic length scale. Finally, given the extensive reports on cooperative effects and ordering of water due to the presence of ions and polyelectrolytes in electrolytes, it may even be conceivable to entertain the idea of a length scale in the problem related to the size of the defect embedded in the medium, be this an ion, a molecule or a particle^{15,17,18,48}. All these considerations point to rather intricate possible microscopic underpinnings of the relevant length scales ξ and λ . System-dependent and therefore non-universal governing length scales suggest that nonlocal electrostatic effects may be ubiquitous and more elaborate in character than previously anticipated.

ACKNOWLEDGMENTS

The authors gratefully acknowledge funding from the European Research Council (ERC) under the European Union’s Horizon 2020 research and innovation programme (No 724180), and Roland Netz for helpful discussions.

AUTHOR DECLARATIONS

Conflict of Interest

The authors have no conflicts to disclose.

DATA AVAILABILITY

All data are available within the article or supplemental information.

¹R. Horn, D. Smith, and W. Haller, “Surface forces and viscosity of water measured between silica sheets,” *Chemical Physics Letters* **162**, 404–408 (1989).

²W. A. Ducker, T. J. Senden, and R. M. Pashley, “Measurement of forces in liquids using a force microscope,” *Langmuir* **8**, 1831–1836 (1992).

- ³G. Trefalt, T. Palberg, and M. Borkovec, “Forces between colloidal particles in aqueous solutions containing monovalent and multivalent ions,” *Current Opinion in Colloid & Interface Science* **27**, 9–17 (2017).
- ⁴A. Klug, R. E. Franklin, and S. Humphreys-Owen, “The crystal structure of tipula iridescent virus as determined by Bragg reflection of visible light,” *Biochimica et Biophysica Acta* **32**, 203–219 (1959).
- ⁵H. Matsuoka, D. Schwahn, and N. Ise, “Observation of cluster formation in polyelectrolyte solutions by small-angle neutron scattering. 1. A steep upturn of the scattering curves from solutions of sodium poly(styrenesulfonate) at scattering vectors below 0.01 Å⁻¹,” *Macromolecules* **24**, 4227–4228 (1991).
- ⁶G. M. Kepler and S. Fraden, “Attractive potential between confined colloids at low ionic strength,” *Physical Review Letters* **73**, 356–359 (1994).
- ⁷Y. Han and D. G. Grier, “Confinement-Induced Colloidal Attractions in Equilibrium,” *Physical Review Letters* **91**, 038302 (2003).
- ⁸M. M. Baksh, M. Jaros, and J. T. Groves, “Detection of molecular interactions at membrane surfaces through colloid phase transitions,” *Nature* **427**, 139–141 (2004).
- ⁹C. Haro-Pérez, L. F. Rojas-Ochoa, R. Castañeda-Priego, M. Quesada-Pérez, J. Callejas-Fernández, R. Hidalgo-Álvarez, and V. Trappe, “Dynamic Arrest in Charged Colloidal Systems Exhibiting Large-Scale Structural Heterogeneities,” *Physical Review Letters* **102**, 018301 (2009).
- ¹⁰S. Wang, R. Walker-Gibbons, B. Watkins, M. Flynn, and M. Krishnan, “A charge-dependent long-ranged force drives tailored assembly of matter in solution,” *Nature Nanotechnology* **19**, 485–493 (2024).
- ¹¹H. Egawa and K. Furusawa, “Liposome Adhesion on Mica Surface Studied by Atomic Force Microscopy,” *Langmuir* **15**, 1660–1666 (1999).
- ¹²G. Silbert, D. Ben-Yaakov, Y. Dror, S. Perkin, N. Kampf, and J. Klein, “Long-Ranged Attraction between Disordered Heterogeneous Surfaces,” *Physical Review Letters* **109**, 168305 (2012).
- ¹³A. A. Kornyshev, A. I. Rubinshtein, and M. A. Vorotyntsev, “Model nonlocal electrostatics. I,” *Journal of Physics C: Solid State Physics* **11**, 3307–3322 (1978).
- ¹⁴D. P. Shelton, “Long-range orientation correlation in water,” *The Journal of Chemical Physics* **141**, 224506 (2014).
- ¹⁵Y. Chen, H. I. Okur, N. Gomopoulos, C. Macias-Romero, P. S. Cremer, P. B. Petersen, G. Tocci, D. M. Wilkins, C. Liang, M. Ceriotti, and S. Roke, “Electrolytes induce long-range orientational order and free energy changes in the H-bond network of bulk water,” *Science Advances* **2**, e1501891 (2016).
- ¹⁶J. Duboisset and P.-F. Brevet, “Salt-induced Long-to-Short Range Orientational Transition in Water,” *Physical Review Letters* **120**, 263001 (2018).
- ¹⁷J. Dedic, H. I. Okur, and S. Roke, “Polyelectrolytes induce water-water correlations that result in dramatic viscosity changes and nuclear quantum effects,” *Science Advances* **5**, eaay1443 (2019).
- ¹⁸J. Dedic, H. I. Okur, and S. Roke, “Hyaluronan orders water molecules in its nanoscale extended hydration shells,” *Science Advances* **7**, eabf2558 (2021).
- ¹⁹J. N. Israelachvili and R. M. Pashley, “Molecular layering of water at surfaces and origin of repulsive hydration forces,” *Nature* **306**, 249–250 (1983).
- ²⁰S. Marčelja and N. Radić, “Repulsion of interfaces due to boundary water,” *Chemical Physics Letters* **42**, 129–130 (1976).
- ²¹M. M. Reif and P. H. Hünenberger, “Origin of Asymmetric Solvation Effects for Ions in Water and Organic Solvents Investigated Using Molecular Dynamics Simulations: The Swain Acidity–Basicity Scale Revisited,” *The Journal of Physical Chemistry B* **120**, 8485–8517 (2016).
- ²²P. Loche, C. Ayaz, A. Schlaich, D. J. Bonhuis, and R. R. Netz, “Breakdown of Linear Dielectric Theory for the Interaction between Hydrated Ions and Graphene,” *The Journal of Physical Chemistry Letters* **9**, 6463–6468 (2018).

- ²³R. Walker-Gibbons, A. Kubincová, P. H. Hünenberger, and M. Krishnan, “The Role of Surface Chemistry in the Orientational Behavior of Water at an Interface,” *The Journal of Physical Chemistry B* **126**, 4697–4710 (2022).
- ²⁴A. Kubincová, P. H. Hünenberger, and M. Krishnan, “Interfacial solvation can explain attraction between like-charged objects in aqueous solution,” *The Journal of Chemical Physics* **152**, 104713 (2020).
- ²⁵Q. Du, E. Freysz, and Y. R. Shen, “Vibrational spectra of water molecules at quartz/water interfaces,” *Physical Review Letters* **72**, 238–241 (1994).
- ²⁶S. Ye, S. Nihonyanagi, and K. Uosaki, “Sum frequency generation (SFG) study of the pH-dependent water structure on a fused quartz surface modified by an octadecyltrichlorosilane (OTS) monolayer,” *Physical Chemistry Chemical Physics* **3**, 3463–3469 (2001).
- ²⁷Y. R. Shen and V. Ostroverkhov, “Sum-Frequency Vibrational Spectroscopy on Water Interfaces: Polar Orientation of Water Molecules at Interfaces,” *Chemical Reviews* **106**, 1140–1154 (2006).
- ²⁸A. Myalitsin, S.-h. Urashima, S. Nihonyanagi, S. Yamaguchi, and T. Tahara, “Water Structure at the Buried Silica/Aqueous Interface Studied by Heterodyne-Detected Vibrational Sum-Frequency Generation,” *The Journal of Physical Chemistry C* **120**, 9357–9363 (2016).
- ²⁹P. A. Bopp, A. A. Kornyshev, and G. Sutmann, “Static Nonlocal Dielectric Function of Liquid Water,” *Physical Review Letters* **76**, 1280–1283 (1996).
- ³⁰P. A. Bopp, A. A. Kornyshev, and G. Sutmann, “Frequency and wave-vector dependent dielectric function of water: Collective modes and relaxation spectra,” *The Journal of Chemical Physics* **109**, 1939–1958 (1998).
- ³¹G. Monet, F. Bresme, A. Kornyshev, and H. Berthoumieux, “Nonlocal Dielectric Response of Water in Nanoconfinement,” *Physical Review Letters* **126**, 216001 (2021).
- ³²A. A. Kornyshev, “Nonlocal electrostatics of solvation,” in *The chemical physics of solvation. Part A, Theory of solvation*, Studies in physical and theoretical chemistry ; 38A, edited by R. R. Dogonadze, E. Kalman, A. A. Kornyshev, and J. Ulstrup (Elsevier, 1985) Chap. 3, pp. 77–118.
- ³³A. Hildebrandt, R. Blossey, S. Rjasanow, O. Kohlbacher, and H.-P. Lenhof, “Novel Formulation of Nonlocal Electrostatics,” *Physical Review Letters* **93**, 108104 (2004).
- ³⁴F. Paillusson and R. Blossey, “Slits, plates, and Poisson-Boltzmann theory in a local formulation of nonlocal electrostatics,” *Physical Review E* **82**, 052501 (2010).
- ³⁵M. Belaya, V. Levadny, and D. A. Pink, “Electric Double Layer near Soft Permeable Interfaces. 1. Local Electrostatic,” *Langmuir* **10**, 2010–2014 (1994).
- ³⁶M. Belaya, V. Levadny, and D. A. Pink, “Electric Double Layer near Soft Permeable Interfaces. 2. “Nonlocal” Theory,” *Langmuir* **10**, 2015–2024 (1994).
- ³⁷E. Chibowski and A. Szcześ, “Zeta potential and surface charge of DPPC and DOPC liposomes in the presence of PLC enzyme,” *Adsorption* **22**, 755–765 (2016).
- ³⁸D. W. R. Gruen and S. Marčelja, “Spatially varying polarization in ice,” *J. Chem. Soc., Faraday Trans. 2* **79**, 211–223 (1983).
- ³⁹D. W. R. Gruen and S. Marčelja, “Spatially varying polarization in water. A model for the electric double layer and the hydration force,” *J. Chem. Soc., Faraday Trans. 2* **79**, 225–242 (1983).
- ⁴⁰M. L. Belaya, M. V. Feigel’man, and V. G. Levadnyii, “Structural forces as a result of nonlocal water polarizability,” *Langmuir* **3**, 648–654 (1987).
- ⁴¹E. Ruckenstein and M. Manciu, “The Coupling between the Hydration and Double Layer Interactions,” *Langmuir* **18**, 7584–7593 (2002).
- ⁴²R. Blossey and R. Podgornik, “Field theory of structured liquid dielectrics,” *Phys. Rev. Res.* **4**, 023033 (2022).
- ⁴³A. A. Rubashkin, “The role of spatial dispersion of the dielectric constant of spherical water cavity in the lowering of the free energy of ion transfer to the cavity,” *Russian Journal of Electrochemistry* **50**, 1090–1094 (2014).
- ⁴⁴P. Jungwirth and D. Laage, “Ion-Induced Long-Range Orientational Correlations in Water: Strong or Weak, Physiologically Relevant or Unimportant, and Unique to Water or Not?” *The Journal of Physical Chemistry Letters* **9**, 2056–2057 (2018).
- ⁴⁵A. A. Kornyshev and S. Leikin, “Fluctuation theory of hydration forces: The dramatic effects of inhomogeneous boundary conditions,” *Phys. Rev. A* **40**, 6431–6437 (1989).
- ⁴⁶S. Leikin and A. A. Kornyshev, “Theory of hydration forces. non-local electrostatic interaction of neutral surfaces,” *J. Chem. Phys.* **92**, 6890–6898 (1990).
- ⁴⁷A. Schlaich, J. O. Daldrop, B. Kowalik, M. Kanduč, E. Schneck, and R. R. Netz, “Water Structuring Induces Nonuniversal Hydration Repulsion between Polar Surfaces: Quantitative Comparison between Molecular Simulations, Theory, and Experiments,” *Langmuir* **40**, 7896–7906 (2024).
- ⁴⁸K. J. Tielrooij, N. Garcia-Araez, M. Bonn, and H. J. Bakker, “Cooperativity in Ion Hydration,” *Science* **328**, 1006–1009 (2010).